15 cm by 15 cm resonator used in our experiments, the ratio is about 10,000 (*19*). It has been emphasized that as τ decreases (so that the system becomes more turbulent), the effects of intermittency should become more pronounced (*20*, *21*). It is unclear whether the nature of the observed structures will change at higher levels of energy throughput or as viscous interactions with the boundaries are modified. An improved system for the study of ripple turbulence is the surface of a levitated sphere of fluid. In this instance, waves scatter only from each other and not a boundary.

REFERENCES AND NOTES

1. W. Heisenberg, *Proc. R. Soc. London Ser. A* **195**, 402 (1948).
2. L. F. Richardson, *Weather Prediction by Numerical Process* (Cambridge Univ. Press, Cambridge, 1922); *Proc. R. Soc. London Ser. A* **110**, 709 (1926).
3. A. N. Kolmogorov, *Dokl. Akad. Nauk. SSSR* **30**, 301 (1941); A. M. Oboukhov; *ibid.* **32**, 19 (1941).
4. L. D. Landau and E. M. Lifshitz, *Fluid Mechanics* (Pergamon, New York, 1955).
5. V. E. Zakharov, V. S. L'vov, G. Falkovich, in *Kolmogorov Spectra of Turbulence* (Springer Berlin, 1992), pp. 33–230.
6. R. Z. Sagdeev, *Rev. Mod. Phys.* **51**, 1 (1979).
7. W. B. Wright, R. Budakian, S. J. Putterman, *Phys. Rev. Lett.* **76**, 4528 (1996); W. B. Wright, thesis, University of California, Los Angeles (1996).
8. H. L. Grant, R. W. Stewart, A. Moilliet, *J. Fluid Mech.* **12**, 241 (1961).
9. U. Frisch and S. Orszag, *Phys. Today* (January 1990), p. 24.
10. A. M. Oboukhov, *J. Fluid Mech.* **13**, 77 (1962).
11. A. N. Kolmogorov, *ibid.*, p. 82.
12. B. Christianson, P. Alstrom, M. Levinsen, *Phys. Rev. Lett.* **68**, 2157 (1992); B. J. Gluckman, P. Marq, J. Bridges, J. P. Gollub, *ibid.* **71**, 2034 (1993).
13. M. Faraday, *Trans. R. Soc.* (1831), p. 299.
14. DLP allows us to independently measure the frequency and wavenumber spectra without invoking strong assumptions such as the Taylor hypothesis [S. G. Saddoughi and S. V. Veeravalli, *J. Fluid Mech.* **268**, 333 (1994).].
15. M. H. Seymour, *Z. Phys.* **C62**, 127 (1994); S. Catani, *Phys. Lett.* **B269**, 432 (1991); W. Bartel *et al.*, *Z. Phys.* **C33**, 23 (1986); G. Arnison *et al.*, *Phys. Lett.* **B123**, 115 (1983); C. Albajar *et al.*, *Nucl. Phys.* **B309**, 405 (1988).
16. C. Foias, O. P. Manley, R. Temam, *Phys. Fluids* **A3**, 898 (1991).
17. R. H. Kraichnan, *Bull. Am. Phys. Soc.* **42**, 53 (1997).
18. A. N. Pushkarev and V. E. Zakharov, *Phys. Rev. Lett.* **76**, 3320 (1996).
19. Even for such a low density of modes, these simulations (*18*) were able to generate the Kolmogorov spectrum.
20. R. H. Kraichnan, in *Turbulence and Stochastic Processes*, J. C. R. Hunt, O. M. Phillips, D. Williams, Eds. (Royal Society, London, 1991); *Phys. Fluids* **10**, 2080 (1967).
21. The issue being addressed here is intermittency in fully developed turbulence, not intermittency in the transition to turbulence [D. J. Tritton, in *Physical Fluid Dynamics* (Van Nostrand Reinhold, New York, 1977), pp. 13–16].
22. P. D. Kaplan, M. H. Kao, A. G. Yodh, D. J. Pine, *Appl. Opt.* **32**, 3828 (1993). The effect of surface slope on the transmission coefficient for diffusing light has been calculated by M. U. Vera and D. J. Durian [*Phys. Rev.* **E53**, 3215 (1996)] and D. J. Durian [*ibid.* **E50**, 857 (1994)].

23. We acknowledge valuable discussions with D. Durian, P. H. Roberts, B. I. Halperin, S. Garrett, R. Keolian, and the Lund high-energy physics group. This research is supported by the U.S. Department of Energy (Division of Engineering and Geophysics) and by NASA (Microgravity Research).

8 August 1997; accepted 17 October 1997

IRAK (Pelle) Family Member IRAK-2 and MyD88 as Proximal Mediators of IL-1 Signaling

Marta Muzio,* Jian Ni, Ping Feng, Vishva M. Dixit†

The interleukin-1 receptor (IL-1R) signaling pathway leads to nuclear factor kappa B (NF-κB) activation in mammals and is similar to the Toll pathway in *Drosophila*: the IL-1R–associated kinase (IRAK) is homologous to Pelle. Two additional proximal mediators were identified that are required for IL-1R–induced NF-κB activation: IRAK-2, a Pelle family member, and MyD88, a death domain–containing adapter molecule. Both associate with the IL-1R signaling complex. Dominant negative forms of either attenuate IL-1R–mediated NF-κB activation. Therefore, IRAK-2 and MyD88 may provide additional therapeutic targets for inhibiting IL-1–induced inflammation.

After binding to IL-1, the IL-1R type I (IL-1RI) associates with the IL-1R accessory protein (IL-1RAcP) and initiates a signaling cascade that results in the activation of NF-κB (*1*–*6*). Substantial similarity exists between the IL-1R signaling pathway in mammals and the Toll signaling pathway in *Drosophila*. Toll shares sequence homology with the cytoplasmic domain of the IL-1RAcP and induces Dorsal activation (a homolog of NF-κB) via the adapter protein Tube and the protein kinase Pelle (*7*–*10*). The recently identified IRAK (IL-1R–associated kinase) is homologous to Pelle (*11*). However, in mammalian cells, additional complexity is thought to exist, because of the observation that multiple protein kinase activities coprecipitate with the IL-1RI (*12*, *13*). Furthermore, given that in *Drosophila* the adapter protein Tube interacts with and regulates Pelle's activity, it is likely that analogous adapter or regulatory molecules might participate in IL-1 signaling.

In order to identify putative additional protein kinases associating with the IL-1R signaling complex, expressed sequence tag databases were searched for sequences homologous to IRAK (*14*, *15*). A novel partial human cDNA was identified that showed significant homology, by Clustall alignment analysis, to both IRAK and Pelle. Screening of a human umbilical vein endothelial cell cDNA library resulted in the isolation of a full-length cDNA clone; analysis of the nucleotide sequence revealed an open reading frame encoding a 590–amino acid protein with a calculated size of 65 kD (Fig. 1A). Given its sequence and functional similarity to IRAK, the molecule was designated IRAK-2. Northern (RNA) blot analysis revealed a single IRAK-2 transcript expressed in a variety of tissues whose size (about 4 kb) was consistent with that of the cDNA (Fig. 1B).

Ectopic expression of IRAK-2 induced NF-κB activation as determined by the relative luciferase activity of an NF-κB–responsive construct. Truncated versions encoding amino acids 1 to 96 [IRAK-2(1-96)] and amino acid 97 to the COOH-terminal end [IRAK-2(97-590)] failed to induce any luciferase activity, which suggests that the integrity of the molecule was essential for its function (Fig. 2A). Deletional analysis has previously shown that an NH_2-terminal truncated version of Pelle analogous to IRAK-2(97-590) is also inactive, which leads to the suggestion that Pelle's recruitment to the plasma membrane through its NH_2-terminal domain is necessary for its subsequent function (*7*). Thus, we tested whether IRAK-2(1-96) or IRAK-2(97-590) could act as dominant negative inhibitors of IL-1R–induced NF-κB activity. Coexpression of IL-1RI and IL-1RAcP (here called IL-1Rs for clarity) strongly induced NF-κB activity. Surprisingly, both IRAK-2(1-96) and IRAK-2(97-590) inhibited IL-1Rs–induced NF-κB activity. A dominant negative mutant version of the downstream kinase NIK that is implicated in IL-1R–

M. Muzio and V. M. Dixit, University of Michigan Medical School, Department of Pathology, Ann Arbor, MI 48109, USA.
J. Ni and P. Feng, Human Genome Sciences, Rockville, MD 20850–9998, USA.

*Present address: Mario Negri Institute, Milano, Italy.
†To whom correspondence should be addressed. Present address: Genentech, South San Francisco, CA 94080, USA. E-mail: dixit@gene.com

induced NF-κB activation (*16*) served as a positive control, and the unrelated adapter molecule TRAF2(298-522) was the negative control (Fig. 2B).

Given the sequence similarity between IRAK and IRAK-2, and the functional involvement of IRAK-2 in IL-1Rs–induced NF-κB activity, we analyzed whether IRAK-2 was recruited to the IL-1R

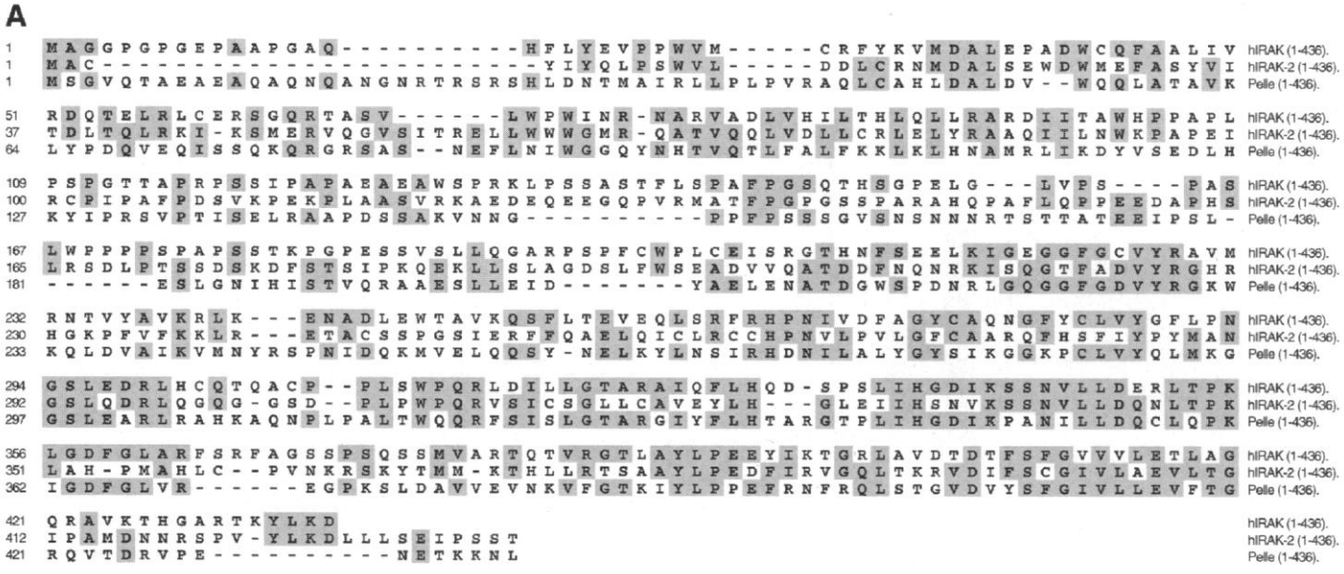

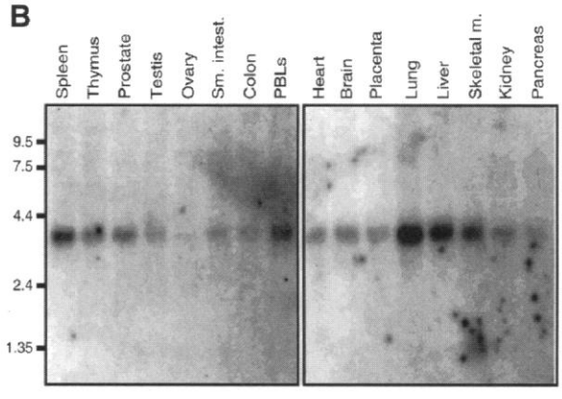

Fig. 1. Sequence analysis and mRNA expression of IRAK-2. (**A**) Sequence alignment of human IRAK, human IRAK-2, and Pelle. Alignment was performed with Clustall software; shading represents identical amino acids. The nucleotide sequence is available from GenBank (accession number AF026273). Residues conserved in protein kinases are shown in bold (*26*). Single-letter abbreviations for the amino acid residues are as follows: A, Ala; C, Cys; D, Asp; E, Glu; F, Phe; G, Gly; H, His; I, Ile; K, Lys; L, Leu; M, Met; N, Asn; P, Pro; Q, Gln; R, Arg; S, Ser; T, Thr; V, Val; W, Trp; and Y, Tyr. (**B**) Detection of IRAK-2 mRNA in adult human tissues. RNA size markers are indicated in kilobases. Adult human multiple-tissue Northern blots (Clontech) were hybridized with a probe corresponding to amino acids 201 to 347 of IRAK-2.

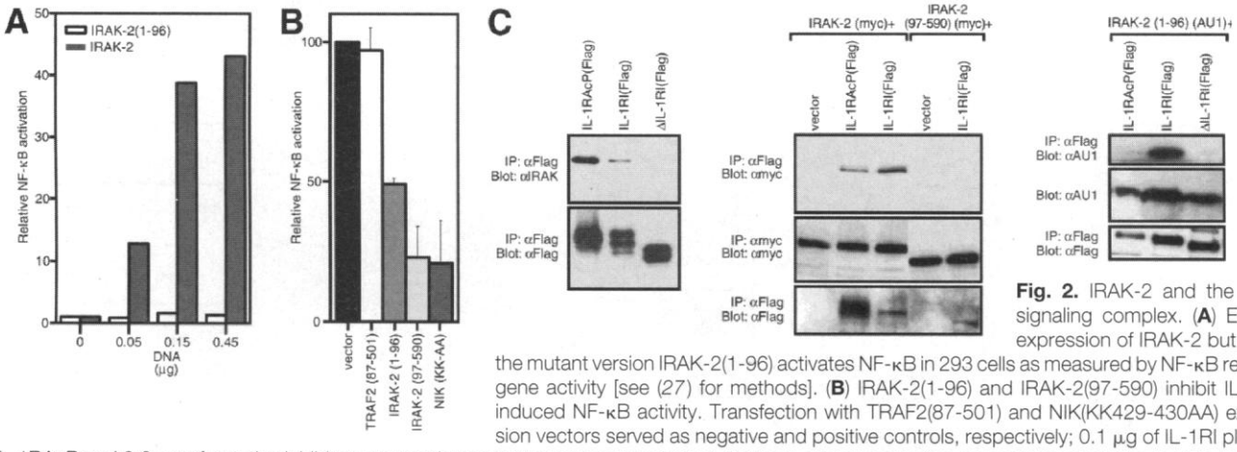

Fig. 2. IRAK-2 and the IL-1R signaling complex. (**A**) Ectopic expression of IRAK-2 but not of the mutant version IRAK-2(1-96) activates NF-κB in 293 cells as measured by NF-κB reporter gene activity [see (*27*) for methods]. (**B**) IRAK-2(1-96) and IRAK-2(97-590) inhibit IL-1Rs–induced NF-κB activity. Transfection with TRAF2(87-501) and NIK(KK429-430AA) expression vectors served as negative and positive controls, respectively; 0.1 μg of IL-1RI plus 0.1 μg of IL-1RAcP and 0.6 μg of putative inhibitory expression constructs were transfected. Data are expressed as the percentage of relative IL-1Rs–induced NF-κB activity. (**C**) IRAK-2 associates with IL-1RI and IRAK associates with IL-1RAcP. 293T cells were transfected with Flag–IL-1RAcP, IL-1RI, or a truncated version of IL-1RI(ΔIL-1RI) as a negative control (*28*) together with the indicated plasmids. The presence of endogenous IRAK, Myc-tagged IRAK-2, and Myc-tagged IRAK-2(97-590) or AU1-tagged IRAK-2(1-96) that coprecipitated with the receptors was detected by immunoblotting with a polyclonal antiserum to IRAK (αIRAK), HRP-conjugated antibody to Myc (αmyc), or antibody to AU1 (αAU1) (*29*).

signaling complex. Although IRAK preferentially coprecipitated with IL-1RAcP, IRAK-2 preferentially bound IL-1RI. A truncated version of IRAK-2 that lacked the first 96 amino acids [IRAK-2(97-590)] did not associate with IL-1RI, which suggests that the NH_2-terminal segment docks with the cytoplasmic domain of IL-1RI. Confirming this, the first 96 amino acids [IRAK-2(1-96)] specifically coprecipitated with IL-1RI (Fig. 2C).

NF-κB activation induced by a number of cytokine receptors is mediated by members of the TRAF adapter family. TRAF2, for example, plays a critical role in NF-κB activation mediated by tumor necrosis factor receptor–1 (TNFR1) and –2 (TNFR2). TRAF6 has been implicated in the IL-1 signaling pathway and has been shown to complex with IRAK (*17*). We therefore determined whether IRAK-2 interacted

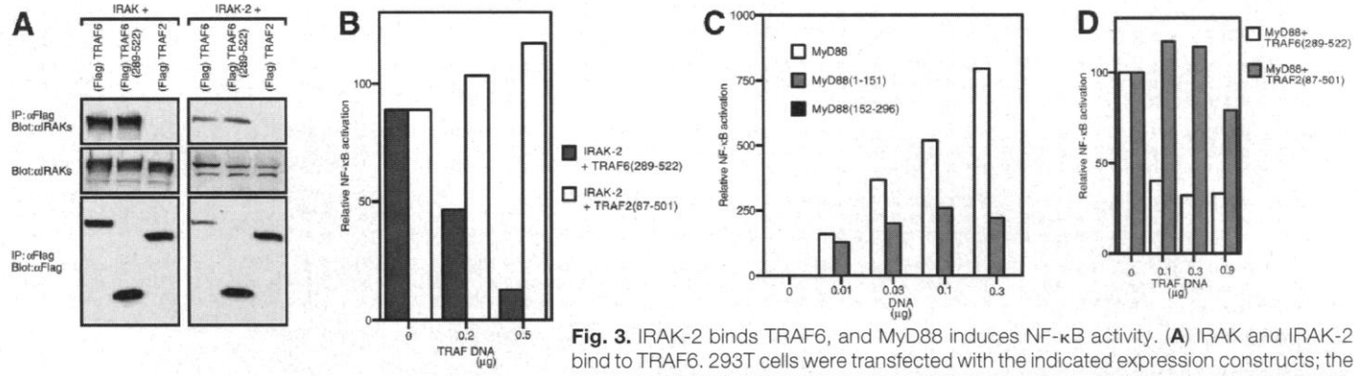

Fig. 3. IRAK-2 binds TRAF6, and MyD88 induces NF-κB activity. (**A**) IRAK and IRAK-2 bind to TRAF6. 293T cells were transfected with the indicated expression constructs; the presence of IRAK (left panel) or IRAK-2 (right panel) in TRAF6 or TRAF2 immunecomplexes was detected with a specific rabbit antiserum to IRAK or IRAK-2. Related TRAF2 was used as a negative control. (**B**) IRAK-2–induced NF-κB activity is specifically abrogated by TRAF6(289-522) but not by TRAF2(87-501). Two hundred ninety-three cells were transfected with 0.2 μg of IRAK-2 and increasing amounts of TRAF constructs. (**C**) Ectopic expression of MyD88 in 293 cells results in the induction of NF-κB activity. A mutant version of MyD88 encoding a NH_2-terminal region [MyD88(1-152)] was similarly capable of inducing NF-κB activity, albeit to a lesser extent; in contrast, a mutant version of MyD88 coding for amino acids 152 to the end [MyD88(152-296)] failed to induce any luciferase activity (not evident in graph). (**D**) MyD88-induced NF-κB activity was selectively inhibited by a dominant negative version of TRAF6 [TRAF6(298-522)] but not by TRAF2(87-501); 0.1 μg of MyD88 and increasing amounts of TRAF expression constructs were used. Data are expressed as the percentage of relative MyD88-induced NF-κB activity.

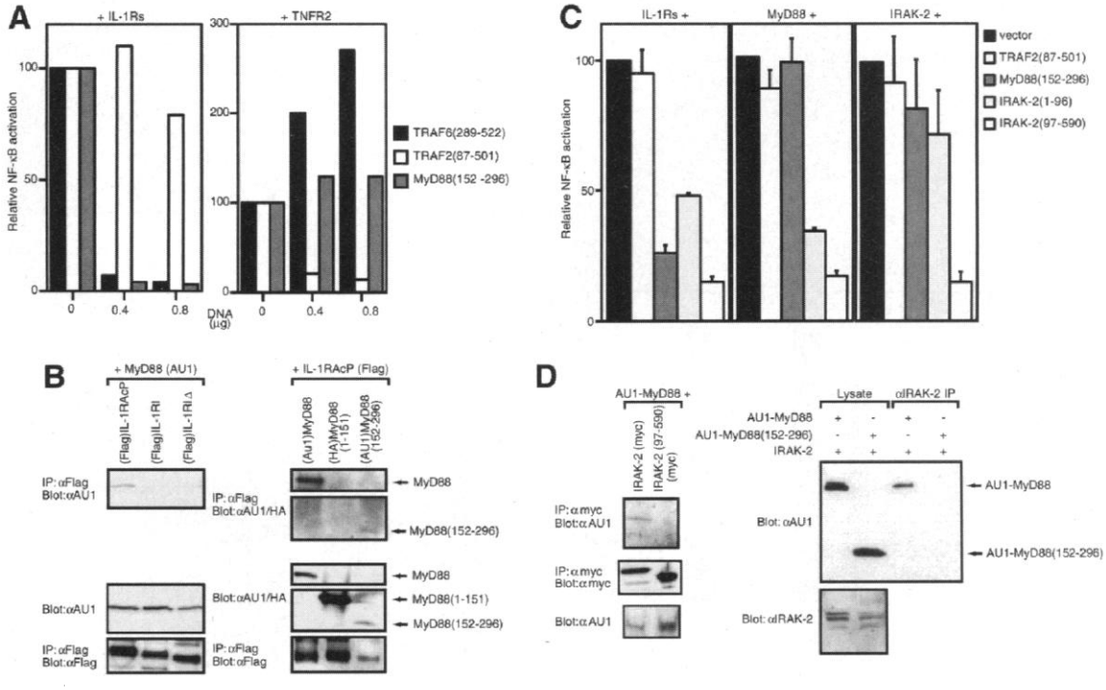

Fig. 4. Molecular ordering of IL-1Rs, MyD88, and IRAK-2. (**A**) MyD88 (106-296) selectively inhibits IL-1Rs– but not TNFR2-induced NF-κB activity. Dominant negative TRAF6(298-522) and TRAF2(87-501) were used as positive controls to inhibit IL-1Rs– and TNFR2-induced NF-κB activity, respectively; 0.5 μg of receptors and increasing amounts of putative dominant negative expression constructs were transfected. Data are expressed as the percentage of relative IL-1Rs– or TNFR2-induced NF-κB activity. (**B**) MyD88 binds IL-1RAcP through a homophilic interaction. 293T cells were transfected with the indicated IL-1Rs and AU1-tagged MyD88 and MyD88(106-296) or HA-tagged MyD88(1-105). MyD88 coprecipitating with IL-1RAcP was detected by immunoblot analysis using a monoclonal antibody to AU1. (**C**) MyD88 dominant negative [MyD88(152-296)] abrogates IL-1Rs–induced but not IRAK-2–induced NF-κB activity. Conversely, IRAK-2 dominant negative versions [IRAK-2(1-96) and IRAK-2(97-590)] significantly inhibit both IL-1Rs– and MyD88-induced NF-κB activity; 0.2 μg of inducer and 0.6 μg of dominant negative expression constructs were used in each transfection. Data are expressed as the percentage of relative induced NF-κB activity. (**D**) MyD88 coprecipitates with IRAK-2 but not with an NH_2-terminal truncated version lacking the first 96 amino acids [IRAK-2(97-590)]. Similarly, NH_2-terminally deleted MyD88—MyD88(152-296)—failed to complex with native IRAK-2.

with TRAF6. Both IRAK and IRAK-2 coprecipitated with TRAF6 but not with the related TRAF2 adapter molecule (Fig. 3A). A dominant negative version of TRAF6 [TRAF6(298-522)], which inhibits IL-1–induced NF-κB activity, bound both IRAK and IRAK-2 (Fig. 3A). IRAK-2–induced NF-κB activity was specifically inhibited by dominant negative TRAF6(298-522) but not by a dominant negative version of TRAF2 [TRAF2(87-501)] (Fig. 3B). Thus, TRAF6 probably acts downstream of IRAK-2.

Collectively, these data suggested that IRAK-2 is a component of the IL-1R signaling complex. It is not yet known whether IRAK and IRAK-2 are functionally redundant but differentially expressed or whether their combined presence modulates IL-1 signaling.

We sought additional proximal adapters and regulators for this pathway by systematically looking for proteins with homology to either Tube or IL-1RAcP. BLAST searches of the public database revealed the cytoplasmic domain of the IL-1RAcP to possess significant homology to MyD88 (*18*). Others have reported sequence similarity between MyD88, IL-1RI, and Toll, but the functional significance of this homology has been obscure. MyD88 has a modular structure: an NH_2-terminal "interaction domain" (or DD for death domain, initially defined in proteins involved in programmed cell death) (*19*, *20*) and a COOH-terminal domain related to the cytoplasmic region of IL-1RAcP, IL-1RI, Toll, and the recently identified human Toll homolog (*21–24*). The presence of these two distinct domains suggested that MyD88 might connect an IL-1R family member with a downstream signaling mediator. To explore this possibility, a functional characterization of human MyD88 was undertaken.

Ectopic expression of MyD88 strongly induced NF-κB activity in a concentration-dependent manner. Similarly, a truncated version of MyD88 encoding the NH_2-terminal domain (DD)—MyD88(1-151)—activated NF-κB, albeit to a lesser extent (Fig. 3C). MyD88-induced NF-κB activity was specifically inhibited by expression constructs of TRAF6 but not by TRAF2 dominant negatives. Therefore TRAF6 and MyD88 probably participate in the same signaling pathway, and TRAF6 functions downstream of MyD88 (Fig. 3D). The COOH-terminal region of MyD88(152-296) did not induce any luciferase activity (Fig. 4A) but could act as a dominant negative inhibitor of IL-1Rs–induced NF-κB activity. MyD88(152-296) specifically inhibited IL-1Rs–induced but not TNFR2-induced NF-κB activation (Fig. 4A).

Given the significant sequence homology between MyD88 and IL-1RAcP, we asked whether the two could interact. On coexpression, MyD88 and IL-1RAcP formed an immunoprecipitable complex. IL-1RI, which shows weaker sequence similarity to MyD88, did not associate with MyD88 under these experimental conditions. Domain mapping studies revealed that the sequence-homologous COOH-terminal region of MyD88 was sufficient to bind to the IL-1RAcP cytoplasmic domain (Fig. 4B), which is in keeping with a homophilic interaction.

To molecularly order the proximal components of the IL-1R signaling complex identified herein, we tested whether a dominant negative version of MyD88 or IRAK-2 could inhibit the active form of the other (Fig. 4C). Dominant negative MyD88 did not inhibit IRAK-2–induced NF-κB activation, but dominant negative IRAK-2 significantly inhibited MyD88-induced NF-κB activity. These results are consistent with MyD88 acting upstream of IRAK-2 in the IL-1R signaling pathway.

Given the presence of a NH_2-terminal interaction domain (DD) in both MyD88 and IRAK-2 (*19*, *20*) we asked whether these two proteins could interact. MyD88 specifically coprecipitated with IRAK-2 (Fig. 4D). A truncated version of IRAK-2 with no NH_2-terminal domain (DD) [IRAK-2(97-590)], which did not induce NF-κB activation, also did not associate with MyD88; similarly, the NH_2-terminal truncated version of MyD88(152-296) that was unable to induce NF-κB activity was also impaired in its ability to bind IRAK-2, lending functional credence to this interaction.

Taken together, these results support a model wherein MyD88 acts as an adapter or regulator in the IL-1R signaling complex by independently interacting with IL-1RAcP and IRAK-2. However, under experimental conditions, we were unable to assemble a complex between MyD88, IRAK-2, and the IL-1Rs. This is consistent with the possibility that MyD88 is only transiently recruited to the IL-1R signaling complex.

Regardless, IRAK-2 and MyD88 are viable therapeutic targets in the IL-1R signaling pathway, which is of paramount importance in inflammatory disease states.

REFERENCES AND NOTES

1. S. A. Greenfeder *et al.*, *J. Biol. Chem.* **270**, 13757 (1995).
2. J. E. Sims *et al.*, *Science* **241**, 585 (1988).
3. C. Korherr, R. Hofmeister, H. Wesche, W. Falk, *Eur. J. Immunol.* **27**, 262 (1997).
4. H. Wesche *et al.*, *J. Biol. Chem.* **272**, 7727 (1997).
5. N. W. Freshney *et al.*, *Cell* **78**, 1039 (1994).
6. M. Martin, G. F. Bol, A. Eriksson, K. Resch, R. Brigelius-Flohe, *Eur. J. Immunol.* **24**, 1566 (1994).
7. R. L. Galindo, D. N. Edwards, S. K. Gillespie, S. A. Wasserman, *Development* **121**, 2209 (1995).
8. J. L. Norris and J. L. Manley, *Genes Dev.* **10**, 862 (1996).
9. A. Letsou, S. Alexander, A. Wasserman, *EMBO J.* **12**, 3449 (1993).
10. J. Grosshans, A. Bergmann, P. Haffter, C. Nusslein-Volhard, *Nature* **372**, 563 (1994).
11. Z. Cao, W. J. Henzel, X. Gao, *Science* **271**, 1128 (1996).
12. A. Eriksson, G. D. Bird, S. K. Dower, *Cytokine* **7**, 649 (1995).
13. R. Singh, T. Guth, M. Konieczkowski, R. Sedor, *J. Clin. Invest.* **100**, 419 (1997).
14. H. Duan and V. Dixit, *Nature* **385**, 86 (1997).
15. M. Tewari *et al.*, *Cell* **81**, 801 (1995).
16. N. L. Malinin, M. P. Boldin, A. V. Kovalenko, D. Wallach, *Nature* **385**, 540 (1997).
17. Z. Cao, J. Xiong, M. Takeuchi, T. Kurama, D. Goeddel, *ibid.* **383**, 443 (1996).
18. K. Lord, B. Hoffman-Liebermann, D. A. Liebermann, *Oncogene* **5**, 1095 (1990).
19. E. Feinstein, A. Kimchi, D. Wallach, M. Boldin, E. Varfolomeev, *Trends Biochem. Sci.* **20**, 342 (1995).
20. K. Hofmann and J. Tschopp, *FEBS Lett.* **371**, 321 (1995).
21. D. Hultmark, *Biochem. Biophys. Res. Commun.* **199**, 144 (1994).
22. G. Hardiman, F. L. Rock, S. Balasubramanian, R. A. Kastelein, J. F. Bazan, *Oncogene* **13**, 2467 (1996).
23. T. Bonnert *et al.*, *FEBS Lett.* **402**, 81 (1997).
24. R. Medzhitov, P. Preston-Hurlburt, C. A. Janeway Jr., *Nature* **388**, 394 (1997).
25. A. Chinnaiyan, K. O'Rourke, M. Tewari, V. Dixit, *Cell* **81**, 505 (1995).
26. S. K. Hanks, A. M. Quinn, T. Hunter, *Science* **241**, 42 (1988).
27. In the NF-κB luciferase assay, cells were transfected with ELAM-Luciferase reporter plasmid (0.1 μg), pCMV-β-galactosidase (β-Gal) (0.2 μg), and the indicated expression vectors; the total amount of transfected DNA was kept constant by supplementation with empty vector. Relative NF-κB activity was calculated by normalizing relative luciferase activity with β-Gal activity as previously described (*17*). Data shown are from one out of three to six independent experiments with similar qualitative results. Data from experiments performed in duplicate or triplicate are expressed as mean ± SE.
28. G. Croston, Z. Cao, D. V. Goeddel, *J. Biol. Chem.* **270**, 16514 (1995).
29. Transfection and coimmunoprecipitation were done as follows. Human embryonic 293 or 293T cells were transiently transfected by the calcium phosphate method with the indicated plasmids. The total amount of DNA was kept constant. Twenty-four to 36 hours after transfection, cells were lysed in 0.5 ml of buffer (1% NP-40, 150 mM NaCl, 50 mM tris, 1 mM EDTA, and protease inhibitors cocktail). Cell lysates were adjusted to 0.7 M NaCl, and the indicated antibodies were added for 1 to 4 hours. Immune complexes were precipitated by the addition of protein G–Sepharose (Sigma). After extensive washing, the Sepharose beads were boiled in sample buffer and the eluted proteins were fractionated by SDS–polyacrylamide gel electrophoresis. Subsequent immunoblotting was performed as described (*25*).

30. M.M. is supported by a Human Frontier Science Program Organization fellowship. We thank Z. Cao for helpful discussions and reagents; I. Jones for help with figures; and D. Chaudhary, A. Chinnaiyan, H. Duan, S. Hu, E. Humke, J. McCarthy, K. O'Rourke, G. Pan, and C. Vincenz for encouragement and discussions.

23 September 1997; accepted 27 October 1997